A

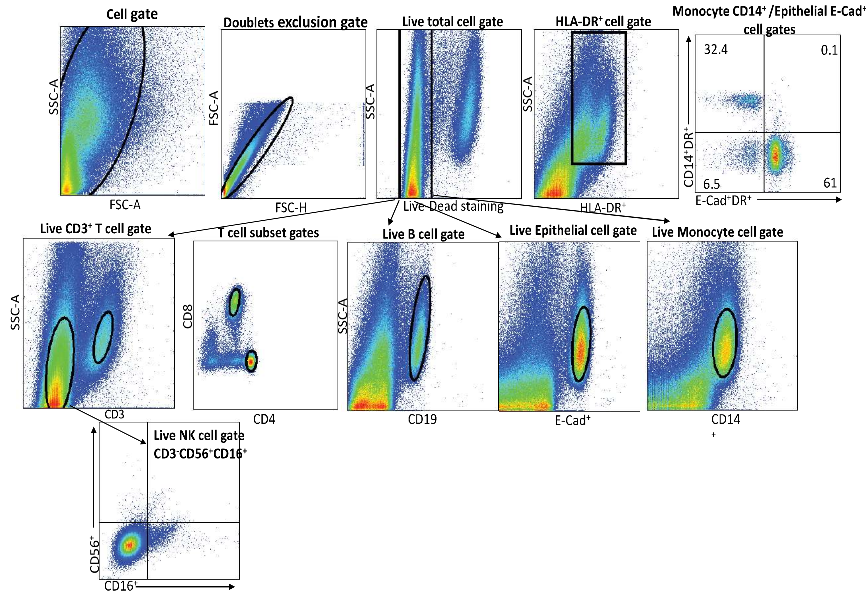

B

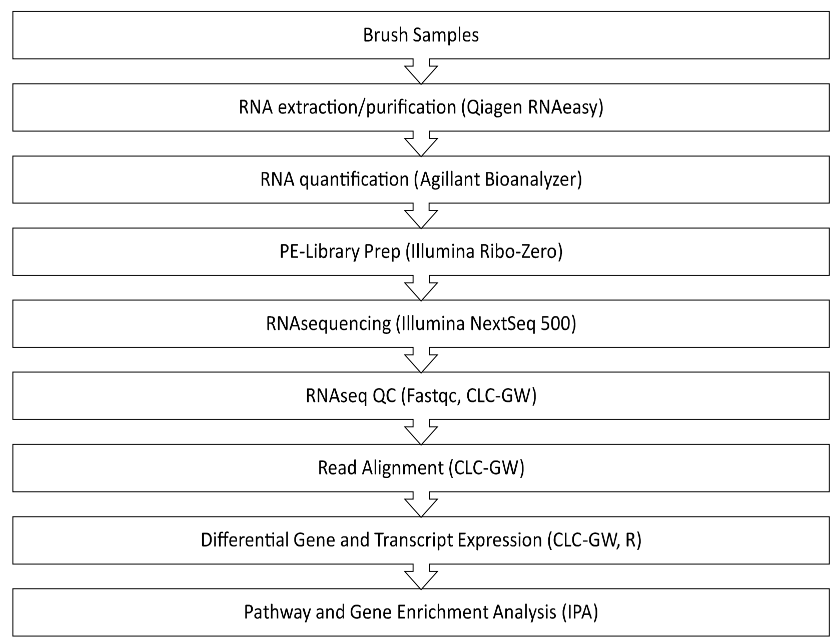

Figure S1. Gating on Airway Brush Cell Populations and RNAseq Pipeline

A) Representative flow cytometric plots of gating strategy to analyze the phenotype of the cells on airway brushes. Gating was done on airway brush cells creating a cell gate on FSC and SSA plot and doublet exclusion based on a FSC-A and FSC-H plot, with singlets inclusion, and live/cells, after we exclude the death cells. Live/Dead Fixable Blue Dead-Cell Stain was used for gating on viable cells. From live cells gate gating was done on HLA-DR+ cells followed by monocytes (CD14+HLA DR+) cells and epithelial cells (E-Cad+ HLA DR+). T cells (CD3+) with CD4+ or CD8+ T cell subpopulations, B cells (CD19), NK cells (CD3-CD56+CD16+) were also gated. Plots are representative from the total of the airway brushes subset of n=12 LTRs. All cells were collected for flow cytometric analysis with a range of 0.5-1x106 total events/condition collected using LSR Fortessa-cytometer with a UV-Laser (BD Biosciences) Data analysis and graphic representations were done with FlowJo v.10 (TreeStar, Ashland, OR). B) Algorithm for RNAseq pipeline analysis.

AL627309.3	SIX3-AS1	MUC13	ATP10B	TRBV7-9	SAA4	ANKRD20A9P	DUOX2	KRT13	VSTM1	U62317.2
MTCO1P12	SIX3	TF	GABRG2	DEFA1	SAA2-SAA4	EPSTI1	DUOXA2	KRT16	KIR3DX1	U62317.5
AJAP1	PLEK	LINC02000	AC034199.1	DEFA3	SAA2	CPB2	C15orf48	SLC4A1	FCAR	KLHDC7B
TNFRSF9	LINC01888	SHOX2	LINC01366	OR7E125P	SAA1	SCEL	AC025580.1	HOXB1	AC245128.3	GLRA2
SLC2A5	DYSF	AC008040.2	SNORA74B	DEFB4A	NAV2-AS1	OR4K2	SCG3	HOXB-AS1	SYT5	AC131011.1
TNFRSF8	LINC01293	CHRD	ADAMTS2	AC011008.2	C11orf96	RNASE2	PRTG	LINC02086	PTPRH	CPXCR1
ARHGEF19-AS1	AC244205.2	AC068631.1	AL512329.2	LGI3	SYT13	CEBPE	AQP9	IGF2BP1	AL121757.1	DRP2
PADI4	IGKC	FETUB	OFCC1	ADAMDEC1	CHST1	GZMH	GCNT3	TMEM100	SNORD17	TCEAL2
PLA2G2D	IGKV4-1	AC007920.2	EDN1	IDO1	MS4A3	GZMB	CSPG4P13	CA4	MYBL2	CLDN2
CDA	IGKV1-5	LINC01983	ASS1P1	AC007991.4	LRRC32	NOVA1	ADAMTS7P3	SOCS3	PI3	AFF2
SMPDL3B	IGKV1-9	FGFBP1	AL049543.1	IDO2	B3GNT6	AL133304.2	BCL2A1	DLGAP1-AS5	MMP9	FATE1
LINC01225	IGKV3-11	NWD2	OR2I1P	TCIM	MYO7A	AL139099.5	AC015871.5	POTEC	SLCO4A1	TKTL1
LINC01226	IGKV3-15	AC111000.4	UBD	ANK1	MMP8	RN7SL1	HAPLN3	LOXHD1	TNFRSF6B	CTAG2
CSF3R	IGKV1-16	CSN1S1	HLA-G	AC131902.1	MMP1	AL133241.1	LINC02207	LIPG	FP671120.3	
DMBX1	IGKV1-17	MUC7	TRIM31	AC091173.1	MMP12	NGB	HBA1	ALPK2	FP236383.2	
PDE4B	IGKV3-20	JCHAIN	LINC00243	AC079209.1	CARD17	SERPINA3	MEFV	OACYLP	FP236383.3	
PTGES3P1	IGKV1-27	CXCL8	DPCR1	IMPA1P1	HTR3A	TCL6	AC138969.2	AC010507.1	TPTE	
VCAM1	IGKV2-30	PF4	CFB	ANXA13	NNMT	AL161669.1	AC008938.1	KF456478.1	SAMSN1	
AMY2A	IGKV1-33	EREG	C6orf222	MTRF1LP2	GRIK4	EXOC3L4	LINC02195	SEMA6B	AF130351.1	
AC092506.1	IGKV1D-39	CXCL9	TREML2	COL22A1	AP004147.1	IGHA2	ZG16	CD70	OLIG2	
EPS8L3	IGKV2D-28	CXCL10	TREML3P	LYPD2	OR8D1	IGHE	ITGAD	TNFSF14	OLIG1	
TMIGD3	LINC00342	CXCL11	PGC	SLURP2	NTM	IGHG4	AC093520.1	AC008878.1	TSPEAR-AS1	
BCL2L15	IL1R2	CXCL13	AL133375.1	AC017067.1	AC006063.2	IGHG2	AC007342.3	FCER2	SMPD4P1	
U1_10	IL18RAP	SPP1	PLA2G7	SPATA31A6	CLEC4C	IGHA1	ADGRG3	TGFBR3L	IGLV4-69	
GJA5	AC140479.7	AC097478.1	TAAR3P	SPATA31A7	SLC2A14	IGHG1	CMTM2	CCL25	IGLV8-61	
S100A9	IL1B	AC108067.1	IL22RA2	LINC01506	SLC2A3	IGHG3	PKD1L2	OR7E25P	IGLV6-57	
S100A12	NCKAP5-IT1	TNIP3	AL591468.1	RORB	CLEC4E	IGHM	FENDRR	AC011472.2	IGLV1-47	
S100A8	CXCR4	IL21	RAET1L	NUTM2F	GRIN2B	IGHV1-2	CA5A	AC008481.3	IGLV1-44	
NPR1	TNFAIP6	IL21-AS1	TAGAP	ORM1	SLCO1B3	IGHV1-3	SLC22A31	SLC5A5	IGLV1-40	
C1orf61	FAP	AC139720.1	MAS1	FUT7	SLCO1B7	IGHV4-4	TUBB3	AC010335.3	IGLV3-25	
FCRL5	XIRP2	AC109811.1	ALG1L5P	IL2RA	SLCO1B1	IGHV2-5	DOC2B	AC123912.2	IGLV2-23	
FCRL3	PTCHD3P2	FGA	IL6	C10orf126	BCAT1	IGHV3-7	LINC02091	MAG	IGLV3-21	
FCRL2	HAGLR	FGG	URGCP-MRPS24	DRGX	SMCO2	IGHV3-11	AC118754.2	FFAR3	IGLV3-19	
OR6N2	CCDC141	RXFP1	AC004847.1	PCDH15	AC009509.1	IGHV3-15	ALOX15B	GPR42	IGLV2-14	
ACKR1	IMPDH1P10	NEIL3	RAMP3	SRGN	LINC02471	IGHV3-21	AURKB	FFAR2	IGLV2-11	
FCGR3B	CTLA4	CLDN22	CCL24	HKDC1	ANKRD33	IGHV3-23	SNORD3A	DPF1	IGLV2-8	
FCRLA	CXCR2P1	F11	DLX6-AS1	PLAU	KRT75	IGHV3-30	MTRNR2L1	LGALS17A	IGLV3-1	
SLAMF6P1	CXCR2	F11-AS1	ZAN	C10orf55	KRT6B	IGHV4-31	CCL2	CLC	IGLL5	
LMX1A	CXCR1	MTNR1A	MUC3A	LIPN	KRT6A	IGHV3-33	CCL7	MIA	IGLC1	
SELL	CCL20	SLC9A3	AC254629.1	LIPM	GPR84	IGHV4-34	CCL8	CEACAM5	IGLC2	
IGFN1	ATP2B2	C7	SERPINE1	ANKRD22	METTL7B	IGHV4-39	HEATR9	CD79A	IGLC3	
IL10	CYP8B1	AC112198.2	RELN	CEP55	LINC02389	IGHV3-48	CCL3	CD177	ADORA2A	
C4BPB	LINC00694	IL31RA	AC004917.1	MKI67	IFNG	IGHV3-49	CCL4	PGLYRP1	UPB1	
C4BPA	CCR3	AC109454.3	SLC26A4-AS1	NLRP6	AC069228.1	IGHV5-51	CCL3L3	PTGIR	OSM	
HSD11B1	CCRL2	SLC25A48	SLC26A4	OR52K1	CMKLR1	IGHV3-53	CCL4L2	IL4I1	C22orf42	
AL606534.2	PROK2	SPINK1	WNT2	HBB	SDS	IGHV4-59	TBC1D3C	KLK7	CSF2RB	
OR2C3	LINC00877	SCGB3A2	LEP	HBG1	RNU4-2	IGHV1-69D	TBC1D3E	AC018755.2	SSTR3	
TRIM58	AC106712.1	CAMK2A	CPA4	OR52N2	HCAR3	IGHV3-72	CSF3	SIGLEC14	APOBEC3A	
OR2M3	ZBED2	SLC36A3	AC083862.2	ADM	AC079949.2	IGHV3-74	AC004585.1	FPR1	Z82214.2	
LINC00211	CD200R1L	NIPAL4	TRBV6-2	AC073172.1	GLT1D1	AC091057.3	KRT38	FPR2	IL17REL	

Figure S2. All genes identified in differential gene expression analysis for CLAD versus non-CLAD LTRs. The 513 included genes had FDR p-value <0.05 and log2 fold-change ≥ 1.5 or ≤ -1.5.

	CLAD no ACR vs Non-CLAD no ACR		CLAD ACR vs CLAD no ACR	
	Fold Change	**FDR p-value**	**Fold Change**	**FDR p-value**
IDO1	15.82	9.27E-9	3.77	0.08
ADAMDEC1	4.53	3.04E-4	4.45	3.21E-3
TNFRSF6B	216.53	2.91E-11	1.82	0.83
SLC5A5	17.85	2.12E-8	-1.31	0.89
MMP9	6.06	1.43E-4	5.89	2.01E-3
SERPINA3	9.01	1.83E-5	-1.07	0.98
IGKC	7.69	1.69E-4	3.63	0.11
IGHA1	5.83	1.12E-3	1.97	0.58
BCL2L15	2.83	1.95E-9	1.31	0.98
MUC13	4.69	3.92E-7	1.27	0.83
C15orf48	3.94	9.85E-4	3.15	0.04
FCAR	6.81	9.82E-5	2.31	0.37
KRT6B	7.25	3.75E-7	-1.43	0.80
MIA	3.16	3.20E-5	1.29	0.79
IGHM	15.53	8.58E-6	4.05	0.15
CXCL9	6.51	1.59E-4	7.87	5.14E-4
CXCL13	15.47	2.19E-4	4.23	0.21
CXCR4	3.05	3.26E-3	3.71	2.84E-3
SAA2-SAA4	5.09	4.73E-6	1.75	0.48
CLC	4.91	0.01	9.81	4.13E-4
SAA2	6.27	3.22E-7	1.09	0.97
ATP10B	3.92	7.62E-6	1.37	0.73
CXCL8	3.63	4.53E-3	3.86	0.01
TCIM	4.19	5.00E-5	1.34	0.83
PTPRH	5.37	1.79E-5	1.30	0.84

Figure S3 – Differential gene expression by CLAD and acute cellular rejection (ACR): A comparison of CLAD no ACR vs non-CLAD no ACR revealed findings very similar to the primary analysis for the top 25 genes. Comparing the CLAD ACR vs CLAD no ACR LTRs found 7/25 of the top genes were upregulated in CLAD with ACR by FDR p-value.

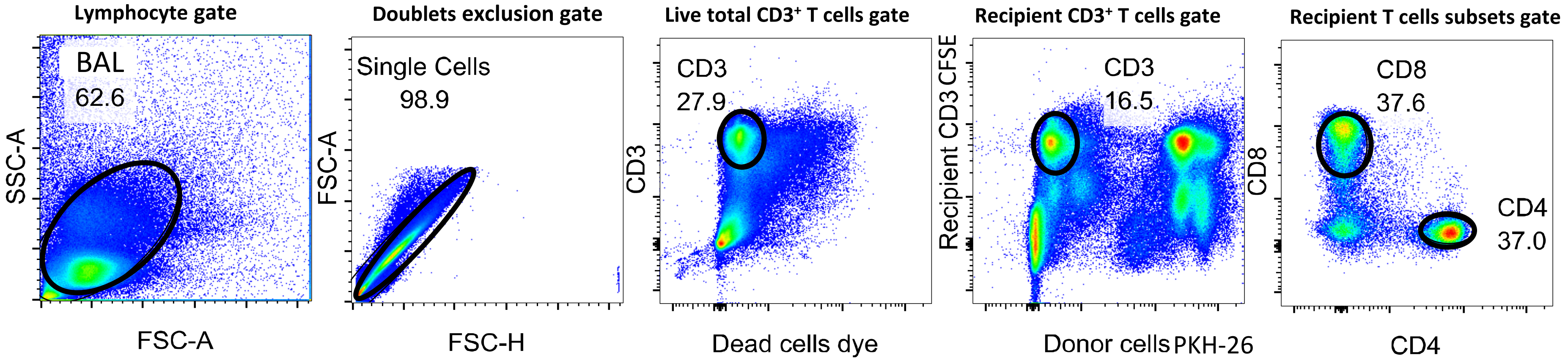

Figure S4: Gating strategy to analyze the allospecific CD8+ or CD4+ T cell alloimmune responses. Representative flow cytometric plots of gating strategy to analyze the allospecific CD8+ or CD4+ T cells from LTR patient. Gating was done on BAL cells creating a lymphocyte gate on FSC and SSA plot and doublet exclusion based on a FSC-A and FSC-H plot, with singlets inclusion, and live/CD3+ T cells, after we exclude the donor cells labeled with PKH-26 (PE channel) dye and gated on recipient live CD3+ labeled with CFSE (FITC channel) and subsequently, the subpopulations of CD4+ or CD8+ recipient T-cells, where the flow plot numbers indicate frequencies (%).
Plots are representative from the subset of n=6 LTRs, with CLAD and n=6 LTRs with non-CLAD. All cells were collected for flow cytometric analysis with a range of 0.5-1x106 total events/condition collected using LSR Fortessa-cytometer with a UV-Laser (BD Biosciences) Data analysis and graphic representations were done with FlowJo v.10 (TreeStar, Ashland, OR).